

9th CIRP Global Web Conference – Sustainable, resilient, and agile manufacturing and service operations :
Lessons from COVID-19

Framework for simulation-based Trajectory Planning and Execution of Robots equipped with a Laser Scanner for Measurement and Inspection

Jan-Philipp Kaiser^{*a}, Sven Norbert Becker^a, Marco Wurster^a, Nicole Stricker^a, Gisela Lanza^a

^a*wbk Institute of Production Science, Karlsruhe Institute of Technology (KIT), Kaiserstr. 12, 76131 Karlsruhe, Germany*

* Corresponding author. Tel.: +1523 9502650; E-mail address: jan-philipp.kaiser@kit.edu

Abstract

Shorter product life cycles require ever faster planning processes for the manufacturing of products. This also applies for measuring processes to ensure compliance with geometric workpiece specifications. In addition, these processes must be designed to be increasingly flexible since mass customization steadily increases product variety. Laser scanning systems mounted on robots offer the possibility of measuring a wide variety of geometries with low measurement uncertainty. In this paper, a method is presented with which measurement trajectories can be planned and virtually validated. We thereby combine and extend existing trajectory planning approaches and explicitly integrate robot kinematics into the planning approach to account for feasibility of the planned trajectories. These can then be directly transferred to the available measurement system. This is enabled by a real time interface directly connecting a virtual environment for measurement simulation and the real measurement system.

© 2021 The Authors. Published by Elsevier B.V.

This is an open access article under the CC BY-NC-ND license (<https://creativecommons.org/licenses/by-nc-nd/4.0>)

Peer-review under responsibility of the scientific committee of the 9th CIRP Global Web Conference – Sustainable, resilient, and agile manufacturing and service operations : Lessons from COVID-19 (CIRPe 2021)

Keywords: Trajectory planning; Robotic; ROS; CoppeliaSim; Laser scanning; Virtual validation; Simulation

1. Introduction

Global trends such as mass individualization, fluctuating demand or the transition towards ever shorter product life cycles make increasingly adaptable production systems inevitable in the future [18]. Planning steps that are necessary to carry out value-adding processes and to produce the products must be run through ever more quickly and frequently. The paradigm of Industry 4.0 creates an opportunity to address these challenges. As hardware becomes less expensive and computing power increases, simulation-based approaches to pre-planning are gaining relevance, especially in industrial settings. Application fields are practically unlimited and can be found in the entire production environment [4], from network planning [3] and production control [5] to production process simulations [1] and simulations with regards to the product in the use phase itself [14].

These approaches can also find application in dimensional metrology. This is especially true for robot-based applications,

where measurement trajectories often need to be specified in advance, such as in ultrasonic testing [9] or optical dimensional surface measurement of workpieces [11]. With regard to optical systems, this results in a wide range of quality criteria for the measuring system that have to be fulfilled, such as compliance with specifications for dimensional measurement, workpiece coverage, spatial reachability and the associated measurability of workpiece properties. Consequently, robot-based quality assurance procedures have to be tested in advance to ensure that they meet these requirements and, if necessary, can be optimized.

Simulation-based validation offers the possibility of increasing time and cost efficiency by saving time- and cost-consuming real experiments since the resources are not occupied during virtual testing. However, existing approaches mostly consider only the solution to a given planning problem and do not sufficiently consider the overall integration into a real production system, which makes fast industrial application difficult so far.

In this work, the problem of trajectory planning of a laser scanning system for surface measurement is considered as an exemplary application. The advantage of these systems compared to conventional tactile coordinate measuring machines

lies in their two-dimensional and fast acquisition. In addition, they offer the necessary flexibility to measure a wide variety of products and, in particular, free-form surfaces. In this work the focus lies especially on the process from the actual planning problem to virtual testing and integration into the real production system.

2. State of the Art

Existing approaches for solving the given planning problem can be roughly subdivided into view-point-based, continuous and volume-based approaches. View-point-based approaches generate view-points (VP) incorporating geometrical sensor specifications. When considering robot-guided laser scanners a VP is, according to [15], a continuous sensor translation perpendicular to the laser fan. The creation process is unique to specific works. Utilizing a sensor model, the covered part of the surface as well as measurement quality prediction (e.g. measurement uncertainty) are attributed to each VP. This is done by extracting a dense and evenly distributed set of points on the workpieces surface and analyzing, which of those are measurable by the VP trajectory. Common approaches and implementations for the view-point-based solution of the planning problem are given in [19], [16], and [2]. These generate much more VP than required for full coverage. Therefore, a selection process is performed. As this problem is formally isomorphic to the set covering problem which is NP-complete, especially greedy algorithms are widespread in the literature. An interesting approach is given by [10] where additionally to the trajectory planning problem via VP, other degrees of freedom such as sensor parameters and spatial workpiece placement are also considered. Continuous approaches partition the workpiece into parameterized surfaces. These surfaces then serve as the basis for generating the required trajectories by creating a path along the shape of the parameterized surface [12]. Volume-based approaches use the mesh of a workpiece to generate the trajectories. In [7] as well as [8], a grouping of triangles of similar normal vectors takes place. These sets of triangles are then used as the basis for generating the trajectories to scan the workpiece. [6] on the other hand, use a voxel-map, where each voxel is assigned a VP in the following.

Analyzing existing literature on automated trajectory planning for surface acquisition and measurement, it is apparent that numerous viable approaches for solving the planning problem exist. Almost all presented approaches allow the solution of the planning problem even under reachability and visibility constraints. These solutions are independent of the workpiece itself, provided that digital product information is available. However, the verification of reachability and feasibility considering constraints, e.g. workspace obstacles as well as the integration of this verification into the planning algorithm are currently insufficiently considered by all of the approaches mentioned above, but are indispensable for a consistent industrial automation concept.

In this paper, we present a fully integrated inspection planning system. Combining and improving conventional VP-based approaches, robotic methods are introduced into the algorithm.

Model-based and with state of the art methods, we verify executability of VP-trajectories and stitch the individual translations into one continuous path. Solutions of the planning system can first be validated in a simulative environment of reality and, in a further step, can be transferred to the real system in a time-efficient manner. In the context of this work, model-based planning problems are considered, assuming the availability of geometry information of the workpieces, for example as CAD files.

The remainder of this work is structured as follows: Section 3 gives an overview of the whole framework and describes the laser scanning model developed in this work. Section 4 introduces the proposed trajectory planner. Chapter 5 presents the results obtained in the simulative environment and chapter 6 summarizes the work and gives an outlook of future work.

3. Development of an environment for model-based trajectory planning

In this work, the software framework *Robot Operating System (ROS)* [17] is used. For validation of the trajectory planning approach, *CoppeliaSim* [13] serves as a virtual environment for simulation.

3.1. Development of a framework for model-based trajectory planning and model-to-real transfer

The framework of the overall setup presented in this work consists of the trajectory planning module, the virtual representation of the real environment in *CoppeliaSim* as well as an interface for model-to-real transfer to ensure rapid transferability and applicability of the trajectories planned in the planning module to a real robot. These are explained in the following:

The **trajectory planning module** itself will be presented in 4. Solutions proposed by the introduced planner meet the following requirements which are:

1. **Reachability:** Planning of collision free trajectories by defining collision objects and solving the inverse kinematic problem using the software framework *MoveIt* integrated in *ROS*.
2. **Visibility:** Checking for visibility of surface points with a given sensor model (see 3.2) using raytracing.
3. **Measurement uncertainty u :** By using a measurement uncertainty model (see 3.2) of the sensors acquisition process the trajectory planner is able to adapt its measurement strategy with compliance to the required measurement specifications of the workpiece. For numeric evaluation, we use the formula introduced in [16]: u is quadratically in the standoff of the laser-scanner (similar to d_{opt} in fig. 4) and reciprocal to the cosine of the incident angle (similar to ψ_{ilt} in fig. 4) w.r.t. the workpiece-surface. We adapt constants in the given formula to our scanning system.

After planning the trajectories of the robot equipped with the sensor system the trajectories can be executed either in the

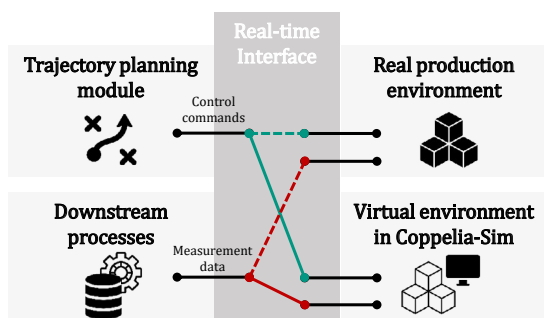


Fig. 1: Visualization of the real-time interface connecting the proposed planning approach with either the simulation in the virtual environment or the real measuring system where measurement output is directed towards downstream processes.

real production environment or in a **virtual environment in CoppeliaSim**. *CoppeliaSim* is a robot simulator, which also allows the integration of various models, like robots, vehicles or moving objects as well as static objects or simple abstracted geometric elements like cubes, to create a realistic validation environment. Therefore validation of the planning process as well as virtual ramp-up of the whole measurement process integrating upstream and downstream processes can be tested and visualized in a realistic virtual environment before transferring it to reality, saving time and resources.

The **real-time interface** developed in this work serves as a real time switch for sensor and actuator inputs and outputs. Inputs for actuators e.g. robot joint commands and the output of sensors e.g. point clouds captured by a laser scanner can be either mapped to and from a simulative environment or the real world. The general workflow is illustrated in 1. Outputs of the trajectory planning module e.g. robot joint commands can be either mapped towards the simulated environment in *CoppeliaSim* or the real world. In return, sensor outputs, e.g. current robot joint angles as well as sensor measurements, e.g. point clouds, are mapped accordingly. For downstream software modules using the simulated or real outputs there is no difference whether these are generated by the simulation of the acquisition process in the virtual environment or reality. Therefore a direct validation and metrological evaluation of the planned trajectory and fast integration in existing workflows in the real world is possible.

3.2. Development of a general and adaptable sensor model for laser scanners

In order to simulate the acquisition process of a laser scanner in a virtual environment as well as during the planning process, an adaptive sensor model is designed, which models the characteristic acquisition properties of a laser scanner in a parameterizable manner. By variation of specific geometric and metrologic parameters of the model, it can be applied to all laser scanners that utilize light-sectioning methods. Such a laser scanner consists of two main components. The first is the laser source, referred to below as the emitter, which projects the two-

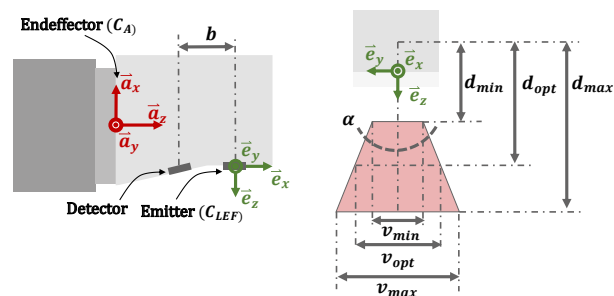


Fig. 2: Visual representation of the sensor model and its parameters used in this work.

dimensional laser line onto the workpiece by dilating a laser beam into a fan. The other is the detection optics, hereinafter referred to as the detector, which is offset to the emitter and detects the illuminated line on the workpiece. Using mathematical methods of triangulation, the coordinates of the projected line are calculated in the sensors reference frame. The main characteristics of the sensor model are shown in figure 2 and summarized in table 1. These are explained in more detail below.

To describe the field-of-view (FOV) and the working range of the sensor, the parameter α is defined as the aperture angle of the laser fan, and d_{min} , d_{opt} and d_{max} as the minimum, optimal and maximum working standoffs in z-direction. With these parameters a direct calculation of the width v_x of the fan at a given working distance in z-direction is possible. We introduce a laser-emitter-frame at the tip of the isosceles fan-triangle as follows: The z-axis lies within the center of the FOV, the x-axis perpendicular to this fan pointing away from the detection optics and the y-axis follows from right-handedness. If we then also know the position of the detector as its x-coordinate b with respect to C_{LEF} , we are able to model the visibility aspect. To check if a point is visible from the current sensor pose manifested in C_{LEF} , we first decide if it lies within the FOV by means of simple geometry and then perform double ray-tracing from C_{LEF} and the detector position towards this point. If visible, we can address the prediction of the measurement uncertainty of this point. This process is done virtually and therefore feasible for the planning algorithm. We chose to use the formula for the prediction of the expected measurement uncertainty u given by [16]. To carry out initial validation tests (see 5), the coefficients of the precision model were only determined approximately within the scope of this work. An exact calibration of the precision model to the existing sensor will be carried out in subsequent work. We do not yet consider effects on u arising from registration of the digitally investigated points in a global reference, e.g. by using forward kinematics. It should be noted that, in addition to the actual parameters of the sensor model for trajectory planning, the transformation between the end effector of the robot C_A and C_{LEF} also plays an essential role, especially for checking reachability of different sensor poses, but strictly speaking it should not be integrated into the sensor model, as this also depends on the coupling elements used.

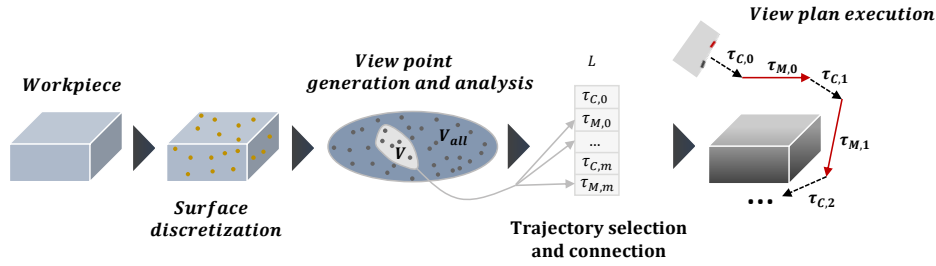


Fig. 3: Overview of the steps of the trajectory planning approach.

Table 1: Parameters of the adaptable sensor model

Parameter description	Variable
Aperture angle of the laser fan	α
Minimal standoff of the scanner in C_{LEF} -z-direction	d_{min}
Optimal standoff of the scanner in C_{LEF} -z-direction	d_{opt}
Maximal standoff of the scanner in C_{LEF} -z-direction	d_{max}
Projected distance of emitter and detector on C_{LEF} 's x-axis	b

4. Integration of a trajectory planning approach into the virtual environment

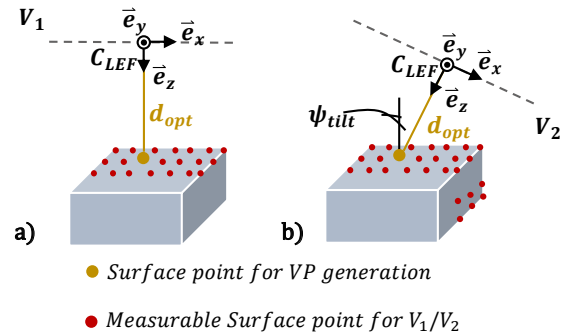
Before the actual planning can take place the workpiece surface is partitioned into measuring points (see 4.1). Then VP are generated based on the points and the measurability of the workpiece surface is analyzed in each case, explicitly taking into account the geometric kinematic constraints of the robot (see 4.2). After the VP for inspection have been determined (see 4.3), the respective individual VP trajectories are sorted and connected (see 4.4). After planning, the inspection can be performed in a controlled manner by the real robot. An overview of the proposed steps of the approach is illustrated in figure 3.

4.1. Model preprocessing

A part of the workpiece surface is permanently covered by the fixture. In this work, the typical case is considered in which the workpiece is supported from underneath, e.g. by placing it on a table-top plane [19]. Consequently, all triangles of the virtual workpiece mesh whose normals are pointing downwards are not considered in the subsequent calculations. The angle Θ between the negative table top normal and the workpiece normal must be greater than this critical angle so that the corresponding workpiece surface can be declared measurable. The reduced surface is then discretized with a specifiable density ρ_S using rejection sampling. The result is a set of n sampled points $S = \{s_1, s_2, \dots, s_i, \dots, s_{n-1}, s_n\}$ on the surface of the workpiece.

4.2. Sampling of measurement trajectories

Based on each $s_i \in S$, multiple VP are generated and analyzed profoundly resulting in the set of all possible VP V_{all} . In general, it is assessed which sample points are measurable from each VP $\in V_{all}$ at which measurement uncertainty and to what

Fig. 4: Simplified visualization of the VP generation process. (a) VP generated with $\delta_{rot} = 0$, $\theta_{tilt} = 0$ and $\psi_{tilt} = 0$. (b) VP generated with $\delta_{rot} = 0$, $\theta_{tilt} = 0$ and $\psi_{tilt} \neq 0$.

extent the trajectory is executable by the robot in the workspace. Based on a surface sample s_i an arbitrary number of VP can be constructed with the following steps (see figure 4):

1. construction of a general C_{LEF} on the surface point s_i with the z-axis pointing towards the negative direction of the surface normal on s_i .
2. rotation of C_{LEF} with fixed angles δ_{rot} , θ_{tilt} and ψ_{tilt} around its z-, x- and y-axis respectively, where δ_{rot} does not change the viewing direction of the given VP however θ_{tilt} as well as ψ_{tilt} enable a tilting of the viewing direction. The tilting in two dimensions introduces a new way of VP-generation compared to previous works; in [2], this process is only carried out in one plane.
3. translation of C_{LEF} in z-direction by a fixed value in the range of d_{min} to d_{max} resulting in the final pose of C_{LEF} . For simplicity a constant value of d_{opt} was chosen in this work.
4. construction of an infinite linear trajectory along the x-direction of the C_{LEF} . During trajectory execution the orientation of C_{LEF} remains the same and just its position is moved.

To constrain the calculated trajectory path into feasible boundaries, the set of all samples $\in S$ that can be measured by the trajectory path is calculated. To do so, we apply the scheme explicated in subsection 3.2 to all sample points and compare the resulting u with a given threshold $u_{max,valid}$. Using the pro-

jection of the two most deflected measurable sample points on the x-axis of C_{LEF} , the calculation of reasonable terminal points of the trajectory is possible. We additionally add a constant extension on both ends since the sampled surface points s_i most likely do not lie on the edges of the workpiece.

With the endpoints and the constant sensor-orientation established, the VP trajectory is fully described. Given the VP trajectory, the robot trajectory τ_M consisting of time-parameterized joint commands can be calculated. We use *MoveIt's* 'cartesian path' planner to generate straight and collision free trajectories since all workspace obstacles are provided to the planner. In many cases, the entire VP trajectory cannot be executed by the robot. In this case, the partial VP trajectory is still considered, provided that it exceeds a certain length $t_{abs,min}$. For each VP, the calculated robot trajectory is stored as well as the measurable surface points including their metrological evaluation.

4.3. Solving the set covering problem

Since in general only a small subset V of V_{all} is needed for inspection, a selection is necessary. For this purpose, the use of a measurability matrix M has proven useful in literature. The columns represent VP and the rows surface samples points. An entry in M is binary coded: If 1, the sample in the elements's row can be measured by the VP of its column. The optimization to be performed can be expressed as solving the well-known Set Covering Problem (SCP), where the solution of this problem satisfies the following constraint: Achieve coverage of all sampled points s_i in S . So the union of the measurable samples of each $VP \in V$ must be equal to S . We formulate the objective literally: Minimize the overall predicted average measurement uncertainty of all $VP \in V$. The direct digital solution procedure represents integer linear programming (ILP), which performs the optimization completely but is time intensive. For run-time purposes we implemented the selection process using a greedy structure as recommended by [19], [16] and [2] as a suitable SCP solution method for trajectory planning problems. In short, the algorithm iteratively puts the $VP \in V_{all}$ into V which has the most 1s in M 's rows that are not yet covered by the VP already in V . In the rare case that multiple VPs are to be put into V , the subselection proposed by [2] is brought to use. This method compares the maximum measurement uncertainty predictions for all the samples assigned to each VP and then picks the one with the lowest value.

4.4. Stitching of optimal trajectories

The set V contains the VP needed for inspection, each of which already carries a measurement trajectory τ_M . The next step is to sort and connect those VP trajectories, so that the inspection can be performed in short time. Therefore, we again propose a greedy structure. This is implemented by introducing an execution list L of sequentially executable VP trajectories. In each iteration step, connection trajectories are calculated between τ_M of L 's last element and both terminal poses of τ_M for all $VP \in V$. A probabilistic roadmap algorithm considering workspace obstacles is employed to find executable connection trajectories. From all those connection trajectories, the one with

the shortest execution time becomes selected and the associated VP is removed from V and pushed back to L . In this transferred VP, we also store this connection path as τ_C . To initialize the algorithm, we use the current pose of the real robot as a pseudo endpose of τ_M so that τ_C of the first attached VP can directly be executed. The program terminates when V is empty. Hence, the inspection can be performed by alternating execution of τ_C and τ_M for each element $\in L$.

5. Results

We applied our algorithm to a scanning system consisting of an UR10e from Universal Robots as a robotic manipulator with the scanner ZEISS T-SCAN 10 mounted as an end effector. We used our developed simulation framework in *CoppeliaSim* for validation. From data sheets, we derived the parameter set for the laser scanner found in table 1.

For testing, a modified cylinder with a total surface area of ca. $0.1m^2$ as product was used to be measured. We chose this round geometry to evaluate the performance of straight VP trajectories on oppositely formed shapes. This object also has a dominant groove with different angles on the lateral surfaces to investigate performance on workpieces that do not embody convex hulls, which is most likely the case in industrial application.

The planner was run with different configurations. We compared different sampling density as well as non enabled tilting ($\delta_{rot} = \theta_{tilt} = \psi_{tilt} = 0$) and enabled tilting (sampling of δ_{rot} , θ_{tilt} and ψ_{tilt}). The amount of generated VP ranged between 73 (low density sampling with $\rho_S = 0.001$ without tilting) and 24570 (high density sampling with $\rho_S = 0.01$ and enabled tilting). In figure 5, it can be observed that the straight shape of the VP's trajectories has proven feasible for the circular test object. However, the result largely depends on the sampling density S which has a profound impact on the result. As only surface regions covered with a sample $\in S$ are considered during planning, coverage issues emerge especially if the density is set too low. Comparing the results with and without the advanced tilting, it can be observed that significant improvements regarding coverage can be achieved. Especially lateral surfaces that are difficult to measure due to the bistatic sensor principle can only be detected when tilting is activated. However, also for a high density and tilting activated, still minor coverage issues exist.

Table 2: Application parameters

(a) Sensor		(b) Planner	
Variable	Value	Variable	Value
α	31 [°]	ρ_S	0.01, 0.005, 0.001 $\left[\frac{points}{mm^2} \right]$
d_{min}	127[mm]	Θ	20 [°]
d_{opt}	182[mm]	$u_{max,valid}$	100[μm]
d_{max}	227[mm]	$t_{abs,min}$	50[mm]
b	76[mm]	δ_{rot}	$\in [0, 360]$ [°]
		θ_{tilt}	$\in [-45, 45]$ [°]
		ψ_{tilt}	$\in [-45, 45]$ [°]

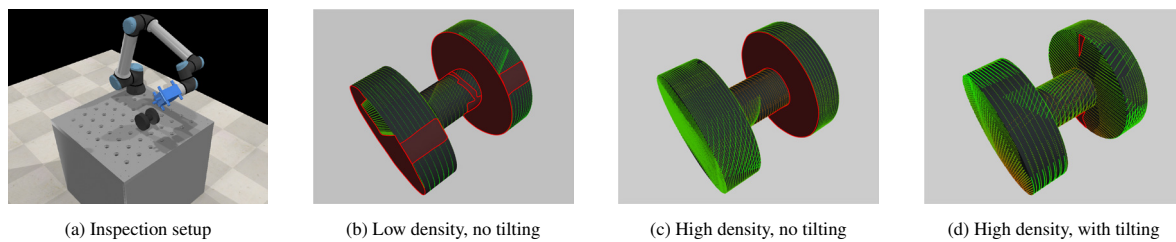


Fig. 5: Setup of inspection station and simulated measurement output as dots (red areas mark non-covered regions)

We believe that this can be overcome by increasing the density even more.

In general, the computing time for planning strongly rises by enabling tilting and by increasing the sampling density. The planning of the path resulting in figure 5d took approximately 24 minutes on a computer equipped with an AMD™ Ryzen 7 1800X and 16 GB RAM as in contrast to the result in figure 5b which only took a few seconds.

6. Conclusion and Outlook

This paper presents an integrated approach to planning measurement trajectories of a laser scanning system. The novelty results from the integration of existing approaches into a holistic planning approach. The developed planning approach enables a trajectory planning under the boundary conditions of reachability, visibility and measurement uncertainty. The result of the planning is a trajectory which is used to carry out a measurement, that in particular takes into account the available working space, due to the inclusion of all objects in the vicinity of the measuring system. Furthermore, the validation of the entire system is possible through the simulation of the acquisition process in a virtual environment which is especially important for virtual ramp-up of processes. By means of tests on a test object through simulation in the virtual environment, the applicability of the planner is shown and the results are discussed.

In future work, the transfer to real application cases will be tested. Deviating from the virtual test object, real components are to be measured and the measurement uncertainty prediction of the planning algorithm will be compared with actually occurring uncertainties in the measurement process. If necessary, this will be followed by a refinement of the measurement uncertainty model of the sensor used. Additionally, it is planned to integrate generation of non-linear trajectories explicitly taking into account the workpiece surface geometry.

Acknowledgements

The project AgiProbot is funded by the Carl Zeiss Foundation.

References

[1] Galantucci, L., Tricarico, L., 1999. Thermo-mechanical simulation of a rolling process with an fem approach. *Journal of Materials Processing Technology* 92-93, 494–501.

[2] Gronle, M., Osten, W., 2016. View and sensor planning for multi-sensor surface inspection. *Surface Topography: Metrology and Properties* 4, 024009.

[3] Jayant, A., Gupta, P., Garg, S., 2014. Simulation modelling and analysis of network design for closed-loop supply chain: A case study of battery industry. *Procedia Engineering* 97.

[4] Kikolski, M., 2017. Study of production scenarios with the use of simulation models. *Procedia Engineering* 182, 321–328. 7th International Conference on Engineering, Project, and Production Management.

[5] Kuhnle, A., Kaiser, J.P., Theiß, F., Stricker, N., Lanza, G., 2021. Designing an adaptive production control system using reinforcement learning. *Journal of Intelligent Manufacturing* 32.

[6] Lartigue, C., Quinsat, Y., Mehdi-Souzani, C., Guarato, A., Tabibian, S., 2013. Voxel-based path planning for 3d scanning of mechanical parts. *Computer-Aided Design and Applications* 11, 220–227.

[7] Li, L., Xu, D., Niu, L., Lan, Y., Xiong, X., 2019. A path planning method for a surface inspection system based on two-dimensional laser profile scanner. *International Journal of Advanced Robotic Systems* 16, 1729881419862463.

[8] Mahmud, M., Joannic, D., Roy, M., Isheil, A., Fontaine, J.F., 2011. 3d part inspection path planning of a laser scanner with control on the uncertainty. *Computer-Aided Design* 43, 345–355.

[9] Mineo, C., Pierce, S.G., Nicholson, P.I., Cooper, I., 2016. Robotic path planning for non-destructive testing – a custom matlab toolbox approach. *Robotics and Computer-Integrated Manufacturing* 37, 1–12.

[10] Mohammadikaji, M., 2018. Automatic inspection planning for optimizing the surface coverage in industrial inspection, in: *Proceedings of the 2017 Joint Workshop of Fraunhofer IOSB and Institute for Anthropomatics, Vision and Fusion Laboratory*. Ed.: J. Beyerer, KIT Scientific Publishing. pp. 1–14.

[11] Phan, N.D.M., Quinsat, Y., Lavernhe, S., Lartigue, C., 2018. Path planning of a laser-scanner with the control of overlap for 3d part inspection. *Procedia CIRP* 67, 392–397.

[12] Prieto, F., Lepage, R., Boulanger, P., Redarce, T., 2003. A cad-based 3d data acquisition strategy for inspection. *Mach. Vis. Appl.* 15, 76–91.

[13] Rohmer, E., Singh, S.P.N., Freese, M., 2013. CoppeliaSim (formerly v-rep): a versatile and scalable robot simulation framework, in: *Proc. of The International Conference on Intelligent Robots and Systems (IROS)*. www.coppeliarobotics.com.

[14] Sandberg, M., Boart, P., Larsson, T., 2005. Functional product life-cycle simulation model for cost estimation in conceptual design of jet engine components. *Concurrent Engineering: RA* 13, 331–342.

[15] Scott, W., Roth, G., Rivest, J., 2003. View planning for automated three-dimensional object reconstruction and inspection. *ACM Comput. Surv.* 35, 64–96.

[16] Scott, W.R., 2009. Model-based view planning. *Mach. Vision Appl.* 20, 47–69.

[17] Stanford Artificial Intelligence Laboratory et al., 2018. Robotic operating system.

[18] Stähr, T., Englisch, L., Lanza, G., 2018. Creation of configurations for an assembly system with a scalable level of automation. *Procedia CIRP* 76, 7–12. 7th CIRP Conference on Assembly Technologies and Systems (CATS 2018).

[19] Tarbox, G., Gottschlich, S., 1995. Planning for complete sensor coverage in inspection. *Computer Vision and Image Understanding* 61, 84–111.